

Vibration analysis of functionally graded material (FGM) grid systems

Kutlu Darılmaz *

Istanbul Technical University, Civil Engineering Department, Maslak, Sariyer, 34469, Istanbul, Turkey

(Received December 17, 2013, Revised June 30, 2014, Accepted July 27, 2014)

Abstract. The paper considers the free vibration analysis of FGM grid systems. Up to now, very little work has been done on this type of system and the paper aspires to fill this gap. Based on the hybrid-stress finite element formulation free vibration solutions for FGM grid systems of various aspect ratios, different types of gradations functions, and support conditions are determined. The tabulation of these results, not available thus far, should be useful to designers and researchers who may use them.

Keywords: grid system; functionally graded materials; free vibration; hybrid finite element

1. Introduction

Functionally graded materials (FGMs) are inhomogeneous composites characterized by smooth and continuous variations in both compositional profile and material properties. This continuity prevents the material from having disadvantages of composites such as delamination due to large interlaminar stresses, initiation and propagation of cracks at the interfaces and so on. Thus use of structures like beams, plates and shells, which are made for functionally grade materials (FGMs), have found a wide range of applications in engineering such as electronics, optics, biomedicine, and aerospace. To understand the behavior of such systems gained importance.

There have been extensive research carried out in the past years to investigate the behavior and design of FG structures but the literature on the analysis of FG beams is limited when compared with FG plates and shells.

Chakraborty *et al.* (2003) proposed a new beam finite element based on the first-order shear deformation theory to study the thermoelastic behavior of functionally graded beam structures. They carried out static, free and wave propagation analysis to examine the behavioral difference of functionally graded material beam with pure metal or pure ceramic. Ching and Yen (2005) presented numerical solutions for two-dimensional FG solids such as simply supported FG beams using a meshless local Petrov-Galerkin method. They later used the same meshless method to calculate the transient thermoelastic deformations of FG beams under a nonuniformly convective heat supply (2006). Qian and Ching (2004) used a meshless method to study the free and forced vibration of an FG cantilever beam. Xiang and Yang (2008) studied the free and forced vibration

*Corresponding author, Ph.D., E-mail: darilmazk@itu.edu.tr

of an FG beam with variable thickness under thermally induced initial stresses based on the Timoshenko beam theory. Sankar (2001) gave an elasticity solution based on the Euler–Bernoulli beam theory for functionally graded beam subjected to static transverse loads by assuming that Young’s modulus of the beam vary exponentially through the thickness. Şimşek and Kocatürk (2009) investigated the free vibration characteristics and the dynamic behavior of a functionally graded simply supported beam under a concentrated moving harmonic load by using Lagrange’s equations under the assumptions of the Euler–Bernoulli beam theory. Chakraborty and Gopalakrishnan (2003) analyzed the wave propagation behavior of FG beam under high frequency impulse loading, which can be thermal or mechanical, by using the spectral finite element method. Aydogdu and Taskin (2007) investigated the free vibration behavior of a simply supported FG beam by using Euler–Bernoulli beam theory, parabolic shear deformation theory and exponential shear deformation theory. Zhong and Yu (2007) presented an analytical solution of a cantilever FG beam with arbitrary graded variations of material property distribution based on two-dimensional elasticity theory. Ying *et al.* (2008) obtained the exact solutions for bending and free vibration of FG beams resting on a Winkler–Pasternak elastic foundation based on the two-dimensional elasticity theory by assuming that the beam is orthotropic at any point and the material properties vary exponentially along the thickness direction. Kapuria *et al.* (2008) presented a finite element model for static and free vibration responses of layered FG beams using an efficient third order zigzag theory for estimating the effective modulus of elasticity, and its experimental validation for two different FGM systems under various boundary conditions. Yang and Chen (2008) studied the free vibration and elastic buckling of FG beams with open edge cracks by using Euler–Bernoulli beam theory. Li (2008) proposed a new unified approach to investigate the static and the free vibration behavior of Euler–Bernoulli and Timoshenko beams. In a recent study by Yang *et al.* (2008), free and forced vibrations of cracked FG beams subjected to an axial force and a moving load were investigated by using the modal expansion technique. Anandrao *et al.* (2012) studied the free vibration and thermal post-buckling of shear flexible FGM beams using finite element formulation based on first order Timoshenko beam theory by considering classical boundary conditions. Tajalli *et al.* (2013) developed a formulation for Timoshenko beams made of functionally graded materials based on the strain gradient theory, and investigated the static bending and free vibration of a FG simply supported beam. Atmane *et al.* (2011) presented a theoretical investigation in free vibration of sigmoid functionally graded beams with variable cross-section by using Bernoulli–Euler beam theory. Pradhan and Chakraverty (2013) investigated the free vibration analysis of functionally graded material beams subjected to different sets of boundary conditions by using the classical and first order shear deformation beam theories. Li and Batra (2013) derived analytical relations between the critical buckling load of a FGM Timoshenko beam and that of the corresponding homogeneous Euler–Bernoulli beam subjected to axial compressive load for different edge conditions.

The aim of this paper is to study the influence of aspect ratio, number of divisions, type of gradations functions, type boundary conditions on the free vibration of FGM grid systems. Both power law and exponential law are taken for the variation of the material properties through the depth of the beam. A hybrid-stress beam finite element is developed and used in this study.

2. Modeling of FGM properties

Different types of gradations laws are available in the literature. In this study power law and

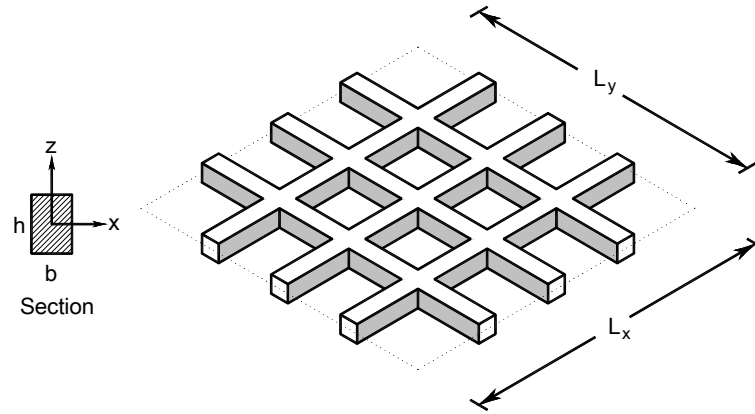


Fig. 1 Functionally graded grid system

exponential law gradation have been considered in order to calculate the material properties of FG structures. FGM consisting of two constituent materials has been considered. The top surface is assumed to be steel and bottom surface is assumed to be Al₂O₃. The region between the two surface consists of a combination of the two materials with continuously varying mixing ratios of two materials.

The power law, for commonly adopted Voight-type estimate, having all the desired properties are introduced by Wakashima *et al.* (1990) is given by

$$P(z) = (P_t - P_b) \left(\frac{z}{h} + \frac{1}{2} \right)^k + P_b \tag{1}$$

$P(z)$ denotes a typical material property (E, G, ρ). P_t and P_b are the corresponding material properties of the top-most and bottom-most surfaces of the beam, and k is the non-negative power-law exponent which defines the material profile through the thickness of the beam.

The exponential law is given by Kim and Paulino (2002)

$$P(z) = P_t e^{-\delta(1-2z/h)}, \quad \delta = \frac{1}{2} \ln(P_t / P_b) \tag{2}$$

It is evident from Eqs. (1) and (2) that when $z = -h / 2, P = P_b$ and when $z = h / 2, P = P_t$.

The typical FGM grid system taken into consideration is depicted in Fig. 1.

3. Finite element formulations

Hybrid-stress finite elements have been developed for the improved analysis based on a modified complementary energy principle in which the intraelement equilibrating stresses and displacements compatible over the entire volume of an element or at the element boundary only are interpolated independently. The element stiffness matrix is obtained using Hellinger-Reissner variational principle in which stresses and displacements are assumed independently, Pian and

Chen (1983), Darılmaz (2012), and Timoshenko beam theory is used. Hellinger-Reissner variational principle establishes the master fields. Two slave strain fields appear, one coming from displacements and one from stresses.

For a typical beam element whose longitudinal axis is x , and y and z are principal centroidal axes, the Hellinger-Reissner functional can be written as

$$\Pi_{HR} = \int_L \{\sigma\}^T [D] \{u\} dx - \frac{1}{2} \int_L \{\sigma\}^T [S] \{\sigma\} dx \quad (3)$$

where $\{\sigma\}$ is the vector of assumed stresses, $[S]$ is the material compliance matrix relating strains, $\{\varepsilon\}$, to stress, $[D]$ is the differential operator matrix corresponding to the linear strain-displacement relations and L is the length of structure

$$\{\varepsilon\} = [s] \{\sigma\} \quad (4)$$

$$\{\varepsilon\} = [D] \{u\} \quad (5)$$

In Eq. (3), the load potential is omitted as it is not required for formulating the element stiffness matrix.

The assumed stress field is described in the interior of the element as

$$\{\sigma\} = [P] \{\beta\} \quad (6)$$

and a compatible displacement field is described by

$$\{u\} = [N] \{q\} \quad (7)$$

where $[P]$ is a matrix which contains the polynomial terms of stress interpolation functions, $[N]$ is a matrix of shape functions, and $\{\beta\}$ and $\{q\}$ are the unknown stress and nodal displacement parameters, respectively.

Intra-element assumed stresses and compatible displacements are independently interpolated. Since stresses are independent from element to element, the stress parameters are eliminated at the element level and a conventional stiffness matrix results. This leaves only the nodal displacement parameters to be assembled into the global system of equations.

Substituting the stress and displacement approximations Eq. (6), Eq. (7) in the functional Eq. (3)

$$\Pi_{HR} = [\beta]^T [G] [q] - \frac{1}{2} [\beta]^T [H] [\beta] \quad (8)$$

where

$$[H] = \int_L [P]^T [S] [P] dx \quad (9)$$

$$[G] = \int_L [P]^T ([D] [N]) dx \quad (10)$$

Now imposing stationary conditions on the functional with respect to the stress parameters $\{\beta\}$ gives

$$[\beta] = [H]^{-1}[G][q] \tag{11}$$

Substitution of $\{\beta\}$ in Eq. (8), the functional reduces to

$$\Pi_{HR} = \frac{1}{2}[q]^T[G]^T[H]^{-1}[G][q] = \frac{1}{2}[q]^T[K][q] \tag{12}$$

where

$$[K] = [G]^T[H]^{-1}[G] \tag{13}$$

is recognized as a stiffness matrix.

The field variables (σ and u) take independent variations for the stationarity of Π_{RH} . The strain vector ε is derived from u using strain-displacement relations. Independently assumed generalized stress field can conveniently be written in terms of axial, shear, torsion and bending actions as

$$\{\bar{\sigma}\}^T = \{N, Q_y, Q_z, M_x, M_y, M_z\} \tag{14}$$

Generalized geometric strain vector derived from displacements can be defined similarly as

$$\{\bar{\varepsilon}\}^T = \{\varepsilon, \gamma_{xy}, \gamma_{yz}, \phi_x, \phi_y, \phi_z\} \tag{15}$$

Utilizing the strain-displacement relations the generalized strain components in the present beam model can be written as

$$\{\bar{\varepsilon}\}^T = \{u'\}, (v' - \theta_z), (w' - \theta_y), \phi'_x, \phi'_y, \phi'_z \tag{16}$$

where the prime indicates differentiation with respect to the axial coordinate x .

The matrices of interpolation functions for element displacements, stress resultants are polynomial function of the coordinate x . For displacement interpolation functions the compatible displacement functions are used. That is with natural coordinate $\xi = 2x / L$, the interpolation functions for two-noded beam element

$$N_1 = (1 - \xi)/2 \quad N_2 = (1 + \xi)/2 \tag{17}$$

For internal force field, the stress parameters are chosen in such a way that the stress equilibrium conditions are satisfied within the element. And also it is recognized that the number of stress modes m in the assumed stress field should satisfy

$$m \geq n - r - p \tag{18}$$

with n the total number of nodal displacements, r the number of rigid body modes and p the number of zero-energy modes in an element. If Eq. (16) is not satisfied, use of too few coefficients in $\{\beta\}$, the rank of the element stiffness matrix will be less than the total degrees of deformation freedom and the numerical solution of the finite element model will not be stable and produces an element with one or more mechanisms.

Increasing the number of β 's by adding stress modes of higher-order term, each extra term will add more stiffness and stiffens the element, Pian and Chen (1983), Darılmaz (2011). Resulting in the least number of parameters the $[P]$ matrix is obtained as

$$[P] = \begin{bmatrix} 1 & 0 & 0 & 0 & 0 & 0 \\ 0 & 1 & 0 & 0 & 0 & 0 \\ 0 & 0 & 1 & 0 & 0 & 0 \\ 0 & 0 & 0 & 1 & 0 & 0 \\ 0 & 0 & x & 0 & 1 & 0 \\ 0 & x & 0 & 0 & 0 & 1 \end{bmatrix} \quad (19)$$

4. Element mass matrix

The problem of determination of the natural frequencies of vibration of a grid system reduces to the solution of the standard eigenvalue problem $[K] - \omega^2[M] = 0$, where ω is the natural circular frequency of the system. Making use of the conventional assemblage technique of the finite element method with the necessary boundary conditions, the system matrix $[K]$ and the mass matrix $[M]$ for the entire structure can be obtained.

Element mass matrix is derived from the kinetic energy expression

$$E_k = \frac{1}{2} \int_L \{\dot{q}\}^T [R] \{\dot{q}\} dx \quad (20)$$

where $\{\dot{q}\}$ denotes the velocity components and $[R]$ is the inertia matrix.

The nodal and generalized velocity vectors are related with the help of shape functions

$$\{\dot{q}\} = \sum_{i=1}^4 [N] \{\dot{q}_i\} \quad (21)$$

Substituting the velocity vectors in the kinetic energy, Eq. (17) yields the mass matrix of an element.

$$E_k = \frac{1}{2} \int_L \{\dot{q}_i\}^T [m] \{\dot{q}_i\} dx \quad (22)$$

$$E_k = \frac{1}{2} \int_L \{\dot{q}_i\}^T [m] \{\dot{q}_i\} dx \quad (23)$$

where $[m]$ is the element consistent mass matrix and is given by

$$[m] = \int_L [N]^T [R] [N] dx \quad (24)$$

Table 1 Properties of metallic (Steel) and ceramic (Al₂O₃) phases

Material	Young's modulus, E (GPa)	Poisons' ratio, ν
Al ₂ O ₃	390	0.25
Steel	210	0.3

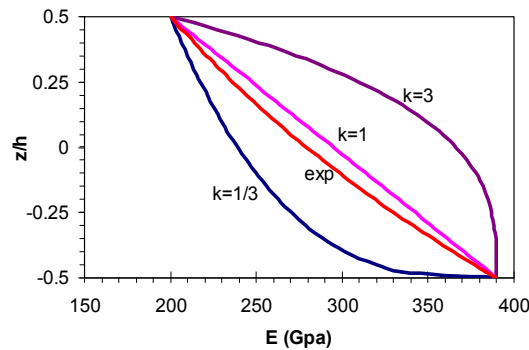


Fig. 2 Variation of the Young's modulus through the thickness of the FG section

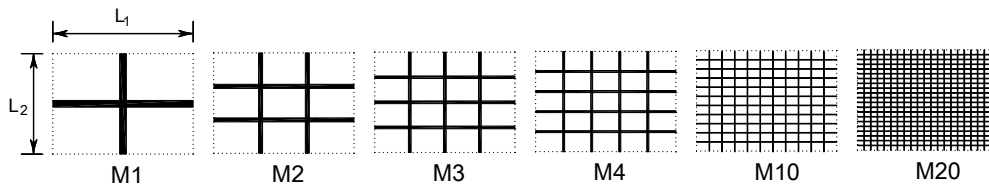


Fig. 3 FGM Grid Systems

5. Numerical results

In this section five different grid systems are considered by using the above formulation to study the influence of aspect ratio (L_1/L_2), type of gradations functions, support condition on the free vibration of FGM grid system. It is assumed that the top and the bottom faces of the beams are steel and Al₂O₃, respectively. The constituent material properties corresponding to each phase are given in Table 1 and constant density is assumed for FGM grid system.

Frequency parameter is non-dimensionalized as $\lambda = (\omega L_1^2 / h) \sqrt{\rho / E_t}$.

It is assumed that the material properties of the beam vary continuously in the thickness direction according to the power-law and exponential form. Fig. 2 shows the variation of Young's modulus of FGM grid system.

Six different grid systems are taken into consideration, Fig. 3. In each case width of the beams is adjusted for keeping the total amount of material constant. For example the width of beam at M4 system is $1/4$ of the width of beam at M1 system. For M1 system the h/b and b/L_1 ratios are 0.5 and 0.1, respectively. Each line segment is modeled by using 20 finite elements. The same mesh is also used for ANSYS solutions.

The numerical examples are conducted for three different aspect ratios, and two different support conditions.

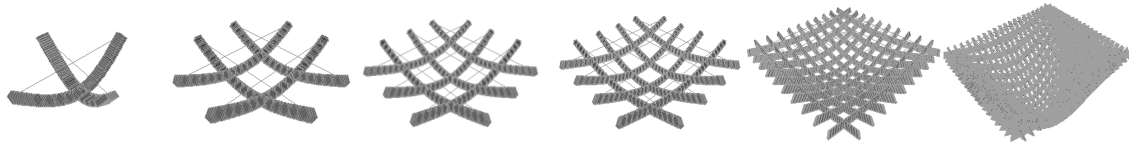


Fig. 4 Typical first mode shape of grid systems ($L_1/L_2 = 1.0$), Simply Supported



Fig. 5 Typical first mode shapes of grid systems ($L_1/L_2 = 1.0$), Fixed

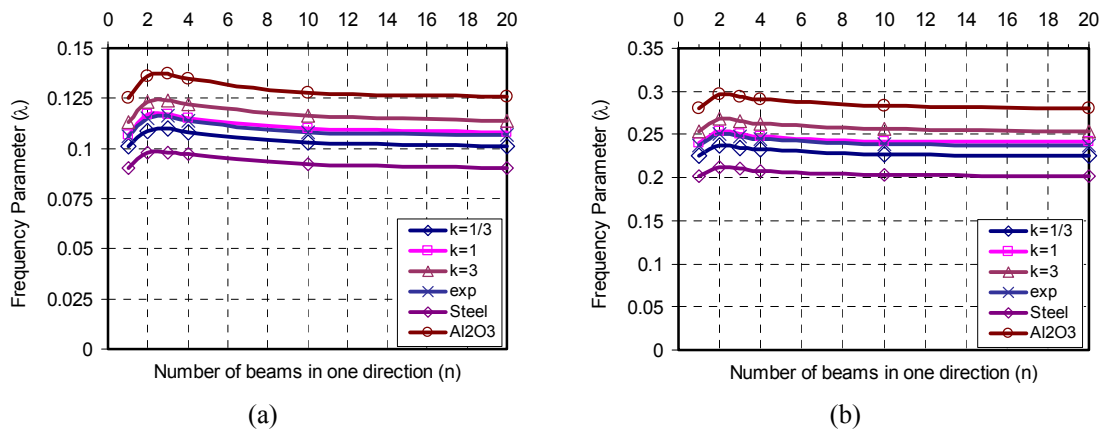


Fig. 6 Variation of frequency parameter λ ($L_1/L_2 = 1.0$), with number of beams in one direction: (a) simply supported; (b) fixed

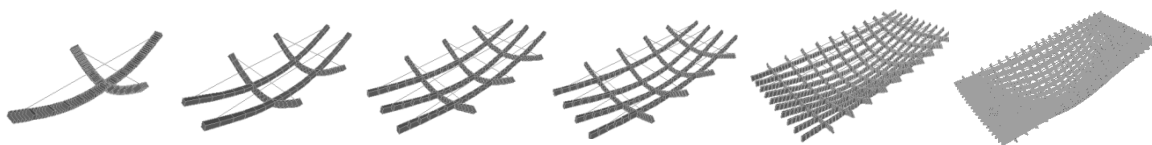


Fig. 7 Typical first mode shape of grid systems ($L_1/L_2 = 2.0$), Simply Supported

Table 2 Frequency parameter λ ($L_1/L_2 = 1.0$), Simply Supported

	$k = 1/3$	$k = 1$	$k = 3$	exp	Steel	Al_2O_3	Steel (ANSYS)
M1	0.101	0.107	0.113	0.106	0.090	0.125	0.089
M2	0.109	0.117	0.123	0.115	0.099	0.136	0.098
M3	0.110	0.117	0.124	0.116	0.098	0.137	0.096
M4	0.108	0.115	0.122	0.114	0.097	0.135	0.094
M10	0.103	0.110	0.116	0.108	0.092	0.128	0.091
M20	0.101	0.108	0.114	0.107	0.090	0.126	0.089

Table 3 Frequency parameter λ ($L_1/L_2 = 1.0$), Fixed

	$k = 1/3$	$k = 1$	$k = 3$	exp	Steel	Al ₂ O ₃
M1	0.225	0.240	0.253	0.237	0.201	0.281
M2	0.237	0.253	0.268	0.250	0.212	0.296
M3	0.235	0.251	0.265	0.248	0.210	0.293
M4	0.233	0.248	0.262	0.245	0.208	0.290
M10	0.227	0.242	0.256	0.239	0.203	0.283
M20	0.226	0.241	0.254	0.238	0.202	0.281

Table 4 Frequency parameter λ ($L_1/L_2 = 1.0$), Simply Supported

	$k = 1/3$	$k = 1$	$k = 3$	exp	Steel	Al ₂ O ₃
M1	0.241	0.256	0.270	0.253	0.215	0.300
M2	0.260	0.277	0.293	0.274	0.232	0.324
M3	0.261	0.279	0.295	0.275	0.233	0.326
M4	0.259	0.276	0.292	0.273	0.231	0.323
M10	0.250	0.267	0.281	0.264	0.223	0.312
M20	0.248	0.264	0.278	0.261	0.221	0.309

Table 5 Frequency parameter λ ($L_1/L_2 = 1.0$), Fixed

	$k = 1/3$	$k = 1$	$k = 3$	exp	Steel	Al ₂ O ₃
M1	0.521	0.555	0.585	0.548	0.465	0.649
M2	0.564	0.601	0.635	0.594	0.503	0.703
M3	0.567	0.604	0.638	0.597	0.506	0.706
M4	0.564	0.601	0.635	0.594	0.503	0.703
M10	0.556	0.592	0.625	0.585	0.496	0.692
M20	0.554	0.590	0.622	0.583	0.494	0.690

Table 6 Frequency parameter λ ($L_1/L_2 = 3.0$), Simply Supported

	$k = 1/3$	$k = 1$	$k = 3$	exp	Steel	Al ₂ O ₃
M1	0.408	0.434	0.458	0.429	0.364	0.508
M2	0.471	0.502	0.530	0.496	0.421	0.587
M3	0.477	0.509	0.538	0.503	0.426	0.595
M4	0.476	0.507	0.535	0.501	0.424	0.593
M10	0.466	0.496	0.523	0.490	0.416	0.580
M20	0.463	0.493	0.520	0.487	0.413	0.576



Fig. 8 Typical first mode shape of grid systems ($L_1/L_2 = 2.0$), Fixed

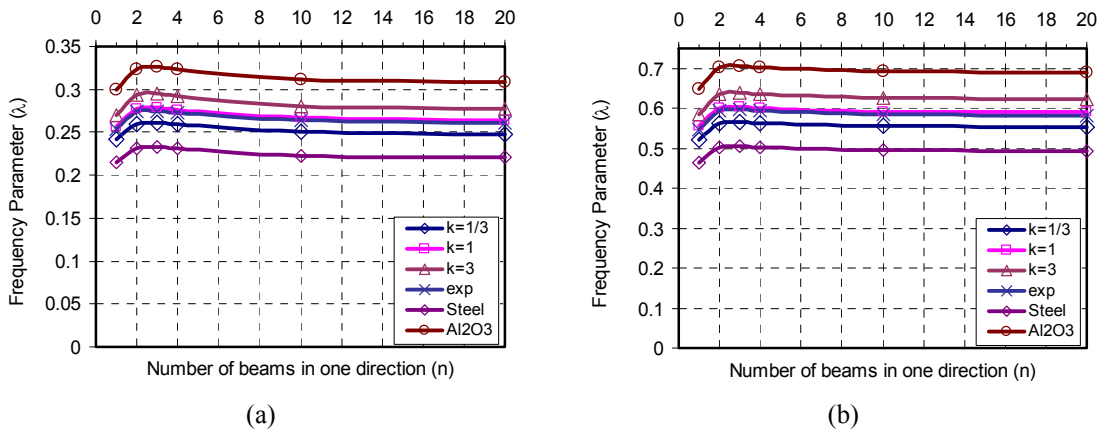


Fig. 9 Variation of frequency parameter λ ($L_1/L_2 = 1.0$), with number of beams in one direction: (a) simply supported; (b) fixed

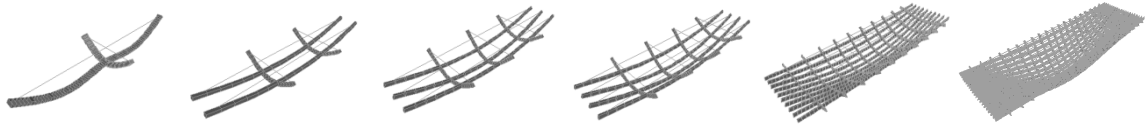


Fig. 10 Typical first mode shape of grid systems ($L_1/L_2 = 3.0$), Simply Supported

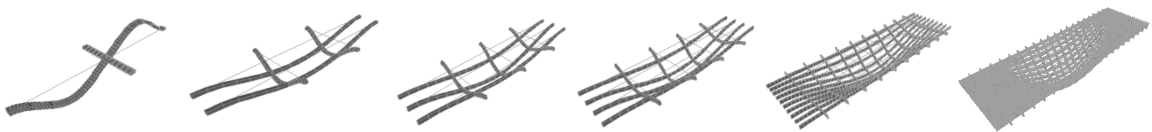


Fig. 11 Typical first mode shape of grid systems ($L_1/L_2 = 3.0$), Fixed

Table 7 Frequency parameter λ ($L_1/L_2 = 3.0$), Fixed

	$k = 1/3$	$k = 1$	$k = 3$	exp	Steel	Al_2O_3
M1	0.722	0.770	0.812	0.760	0.644	0.900
M2	0.967	1.031	1.089	1.018	0.863	1.205
M3	1.028	1.096	1.158	1.083	0.918	1.282
M4	1.038	1.107	1.169	1.093	0.926	1.294
M10	1.037	1.104	1.165	1.091	0.925	1.292
M20	1.035	1.102	1.163	1.089	0.923	1.289

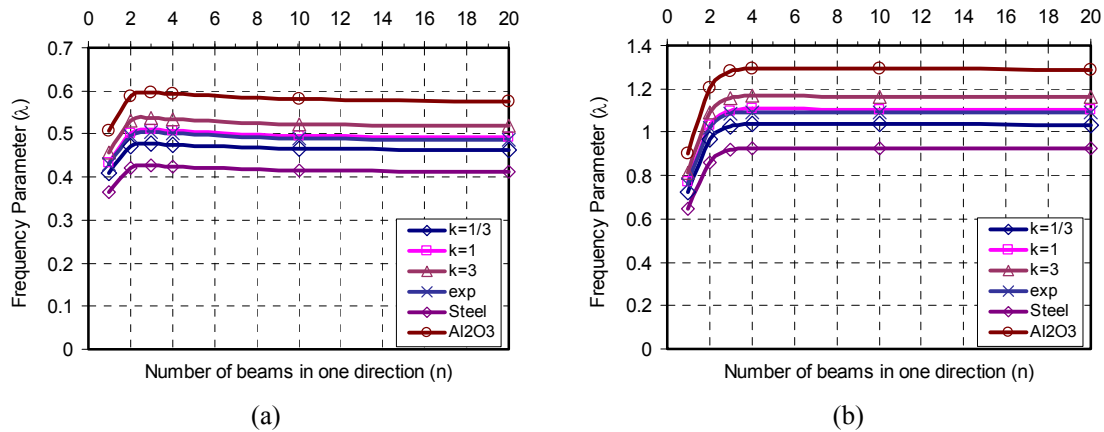


Fig. 12 Variation of frequency parameter λ ($L_1/L_2 = 3.0$), with number of beams in one direction: (a) simply supported; (b) fixed

Variation of frequency parameter (λ) with number of elements (n) in one direction is plotted in Figs. 6, 9 and 12. The first mode shapes are also depicted in Figs. 4, 5, 7, 8, 10 and 11.

Nondimensional frequency parameters, $\lambda = (\omega L_1^2 / h) \sqrt{\rho / E_t}$, are calculated and given in tabular form in Tables 2 to 7.

In order to validate the element behavior for fully steel material, and $L_1/L_2 = 1.0$ aspect ratio, results are compared with ANSYS commercial finite element program results. It can be seen from Table 2 that although the presented element shows a stiffer behavior, the results are found to be in good agreement.

The following observations can be made from the solutions. Individual or combined variation of aspect ratios, material distribution and type of support condition is found to have great influence on the vibration of grid systems.

Frequency parameters obtained from fixed support solutions are higher than the simply support solutions, as expected.

The working range of k are taken as 1/3-3, any value outside this range are producing an FGM having too much of one phase. This can be also observed from the solutions that frequency parameter λ increase with the power-law exponent k . The results are getting closer to the full Al₂O₃ solutions.

It can be observed that among different types of material gradations functions, nondimensional parameter predicted by $k = 3$ are the highest $k = 1/3$ and lowest ones, respectively. For all cases, power law $k = 1$ and exponential function results are close to each other.

It can be observed from the Figs. 10 and 11 for M1 grid system support condition and aspect ratio has a great influence on mode shape. The number of elements has an influence on mode shape in high aspect ratios.

6. Conclusions

An investigation of free vibration of FGM grid systems is presented. The analysis is carried out by using a hybrid stress beam finite element. It is assumed that the material properties of the

beams vary continuously in the thickness direction according to the exponential law and the power-law form. The effects of aspect ratio, type of gradations functions, type of support conditions are discussed. It is observed that the above mentioned effects play very important role on the free vibration behavior of the FGM grid systems. The tables given in this study combines the configurations of grid systems which are mostly used in practice, and will help a practicing engineer to choose an optimum solution considering both economy and other practical limitations.

References

- Anandrao, K.S., Gupta, R.K., Ramchandran, P. and Rao, G.V. (2012), "Non-linear free vibrations and post-buckling analysis of shear flexible functionally graded beams", *Struct. Eng. Mech., Int. J.*, **44**(3), 339-361.
- Atmane, H.A., Tounsi, A., Ziane, N. and Mechab, I. (2011), "Mathematical solution for free vibration of sigmoid functionally graded beams with varying cross-section", *Steel Compos. Struct., Int. J.*, **11**(6), 489-504.
- ANSYS (1997), Swanson Analysis Systems, Swanson J. ANSYS 5.4, USA.
- Aydogdu, M. and Taskin, V. (2007), "Free vibration analysis of functionally graded beams with simply supported edges", *Mater. Des.*, **28**(5), 1651-1656.
- Chakraborty, A. and Gopalakrishnan, S. (2003), "A spectrally formulated finite element for wave propagation analysis in functionally graded beams", *Int. J. Solid Struct.*, **40**(10), 2421-2448.
- Chakraborty, A., Gopalakrishnan, S. and Reddy, J.N. (2003), "A new beam finite element for the analysis of functionally graded materials", *Int. J. Mech. Sci.*, **45**(3), 519-539.
- Ching, H.K. and Yen, S.C. (2005), "Meshless local Petrov-Galerkin analysis for 2D functionally graded elastic solids under mechanical and thermal loads", *J. Compos. Part B: Eng.*, **36**(3), 223-240.
- Ching, H.K. and Yen, S.C. (2006), "Transient thermoelastic deformations of 2D functionally graded beams under nonuniformly convective heat supply", *Compos. Struct.*, **73**, 381-393.
- Darılmaz, K. (2011), "Influence of aspect ratio and fibre orientation on the stability of simply supported orthotropic skew plates", *Steel Compos. Struct., Int. J.*, **11**(5), 359-374.
- Darılmaz, K. (2012), "Analysis of sandwich plates: A three-dimensional assumed stress hybrid finite element", *J. Sandw. Struct. Mater.*, **14**(4), 487-501.
- Kapuria, S., Bhattacharyya, M. and Kumar, A.N. (2008), "Bending and free vibration response of layered functionally graded beams: a theoretical model and its experimental validation", *Compos. Struct.*, **82**(3), 390-402.
- Kim, J. and Paulino, G.H. (2002), "Finite element evaluation of mixed mode stress intensity factors in functionally graded materials", *Int. J. Numer. Meth. Eng.*, **53**(8), 1903-1935.
- Li, X.F. (2008), "A unified approach for analyzing static and dynamic behaviors of functionally graded Timoshenko and Euler-Bernoulli beams", *J. Sound Vib.*, **318**(4-5), 1210-1229.
- Li, S.R. and Batra, R.C. (2013), "Relations between buckling loads of functionally graded Timoshenko and homogeneous Euler-Bernoulli beams", *Compos. Struct.*, **95**, 5-9.
- Pian, T.H.H. and Chen, D.P. (1983), "On the suppression of zero energy deformation modes", *Int. J. Numer. Meth. Eng.*, **19**(12), 1741-1752.
- Pradhan, K.K. and Chakraverty, S. (2013), "Free vibration of Euler and Timoshenko functionally graded beams by Rayleigh-Ritz method", *Compos.: Part B*, **51**, 175-184.
- Qian, L.F. and Ching, H.K. (2004), "Static and dynamic analysis of 2D functionally graded elasticity by using meshless local Petrov-Galerkin method", *J. Chinese Inst. Eng.*, **27**, 491-503.
- Sankar, B.V. (2001), "An elasticity solution for functionally graded beams", *Compos. Sci. Technol.*, **61**(5), 689-696.
- Şimsek, M. and Kocatürk, T. (2009), "Free and forced vibration of a functionally graded beam subjected to a concentrated moving harmonic load", *Compos. Struct.*, **90**(4), 465-473.

- Tajalli, S.A., Rahaeifard M., Kahrobaiyan, M.H., Movahhedy, M.R., Akbari, J. and Ahmadian, M.T. (2013), "Mechanical behavior analysis of size-dependent micro-scaled functionally graded Timoshenko beams by strain gradient elasticity theory", *Compos. Struct.*, **102**, 72-80.
- Wakashima, K., Hirano, T. and Niino, M. (1990), "Space applications of advanced structural materials", ESA SP-303: 97.
- Xiang, H.J. and Yang, J. (2008), "Free and forced vibration of a laminated FGM Timoshenko beam of variable thickness under heat conduction", *J. Compos.: Part B.*, **39**(2), 292-303.
- Yang, J. and Chen, Y. (2008), "Free vibration and buckling analyses of functionally graded beams with edge cracks", *Compos. Struct.*, **83**(1), 48-60.
- Yang, J., Chen, Y., Xiang, Y. and Jia, X.L. (2008), "Free and forced vibration of cracked inhomogeneous beams under an axial force and a moving load", *J. Sound Vib.*, **312**(1-2), 166-181.
- Ying, J., Lue, C.F. and Chen, W.Q. (2008), "Two-dimensional elasticity solutions for functionally graded beams resting on elastic foundations", *Compos. Struct.*, **84**(3), 209-219.
- Zhong, Z. and Yu, T. (2007), "Analytical solution of a cantilever functionally graded beam", *Compos. Sci. Technol.*, **67**(3-4), 481-488.

DL

Nomenclature

b	: width
h	: thickness
k	: power-law exponent
E	: modulus of elasticity
L_1, L_2	: length of the grid system
V	: volume
λ	: frequency parameter
$[D]$: differential operator matrix
$[G]$: nodal forces corresponding to assumed stress field
$[K]$: stiffness matrix
$[N]$: interpolation matrix for displacement field
$[P]$: interpolation matrix for stress
$[S]$: material compliance matrix
$\{q\}$: nodal displacement vector
$\{u\}$: displacement field
$\{\beta\}$: stress parameters
$\{\sigma\}$: stress field
$\{\bar{\sigma}\}$: internal forces
$\{\varepsilon\}$: strain field
$\{\bar{\varepsilon}\}$: strain components
$\{\phi\}$: rotation